Journal of Laser Applications

Investigation on the parameter dependency of the perforation process of graphite based lithium-ion battery electrodes using ultrashort laser pulses

Cite as: J. Laser Appl. **34**, 042003 (2022); https://doi.org/10.2351/7.0000757
Submitted: 20 June 2022 • Accepted: 30 July 2022 • Published Online: 09 September 2022

Max-Jonathan Kleefoot, Jens Sandherr, Marc Sailer, et al.

Journal of Laser Applications ARTICLE scitation.org/journal/jla

Investigation on the parameter dependency of the perforation process of graphite based lithium-ion battery electrodes using ultrashort laser pulses

Cite as: J. Laser Appl. **34**, 042003 (2022); doi: 10.2351/7.0000757
Submitted: 20 June 2022 · Accepted: 30 July 2022 ·
Published Online: 9 September 2022

Max-Jonathan Kleefoot,[1,2] Jens Sandherr,[3] Marc Sailer,[4] Sara Nester,[3] Jiří Martan,[5] Volker Knoblauch,[3] Malte Kumkar,[4] and Harald Riegel[1]

AFFILIATIONS

[1]LaserApplicationCenter (LAZ), Aalen University, Aalen, Germany
[2]Department of Machining Technology, Faculty of Mechanical Engineering (FST), University of West Bohemia, Pilsen, Czech Republic
[3]Institut für Materialforschung Aalen (IMFAA), Aalen University, Aalen, Germany
[4]TRUMPF Laser GmbH, Aichhalder Straße 39, Schramberg, Germany
[5]New Technologies Research Centre (NTC), University of West Bohemia, Pilsen, Czech Republic

Note: Paper published as part of the special topic on Proceedings of the International Congress of Applications of Lasers & Electro-Optics 2022.

ABSTRACT

Perforation of lithium-ion battery electrodes has recently become an increasing interest in science and industry. Perforated electrodes have shown improved electrochemical properties compared to conventional, nonperforated electrodes. It has been demonstrated that through perforation, the fast-charging capability and the lifetime of these batteries can be significantly improved. The electrodes for lithium-ion batteries consist of a copper foil onto which the electrode material is applied as a porous layer. This layer is mainly composed of active material particles, which are bound together by a binder phase. Here, synthetic graphite was used as an active material. Up to now, it has been shown that an advantageous and precise perforation geometry can be produced by ultrashort laser pulse ablation. Since the ablation volumes during perforation of the porous electrode material with ultrashort laser pulses are unusually high compared to solids, this work investigates the parameter dependency on the ablation mechanisms in detail. For this purpose, in particular, single-pulse ablation was investigated with respect to the ablation thresholds at different pulse durations. The pulse durations were varied over a large range from 400 fs to 20 ps. By varying the number of pulses per perforation up to 50 and the single-pulse energy up to 45 μJ, it could be shown that a homogeneous ablation down to the conductor foil through the 63 μm thick active material layer can be achieved.

INTRODUCTION

In order to increase the energy and power density of lithium-ion batteries, research is focusing not only on adapting the cell chemistry but also on the microstructure. A wide range of processes are available for modifying this microstructure. Above all, laser-based processes offer good possibilities for introducing microstructures onto the surface. Microstructural changes in the form of 3D structures,[1] trenches,[2,3] or holes[4,5] have shown significant improvements in the performance of the electrodes.

The laser process increases the surface area and creates transport channels for lithium ions inside the anode.[6] Ionic diffusion pathways inside the active material are, therefore, significantly accelerated.[7] Different simulative and experimental studies showed reduced overpotentials during charging with high currents, leading to enhanced cell capacity retention.[2,5,7] Habedank *et al.* showed a reduction of metallic lithium deposition at the anode surface, which causes the capacity loss during fast charging.[8] Observed improvements were, therefore, demonstrated in terms of lifetime as

well as increased charging and discharging speed.[5] Moreover, Pfleging *et al.* observed enhanced electrolyte wettability for perforated anodes due to capillary forces.[9] In addition to these versatile investigations on the effects of surface modifications on electrodes, the following study focuses on the manufacturing process of laser-perforated electrodes. In our case, the hole shape is defined by crater-like holes. This means that the hole is only perforated through the active material layer. The underlying copper foil should not be damaged. Since the active material particles of an electrode are often thermally sensitive materials, an ultrashort pulse laser with femtoseconds and picoseconds was used. Further advantages of the application of ultrashort pulsed lasers are the high precision and the possibility to produce fine structures.[10,11] In the present study, the laser process for the perforation of commercially used graphite-based electrodes and, especially, the process parameters are to be investigated.

EXPERIMENTAL SETUP

Electrode material

For this study, a standard graphite anode was used as the sample material. Graphite anodes are currently the most common types of anodes on the market and offer advantages such as good theoretical specific capacity. The anode layer consists of a composition of 94 wt. % graphite (SGL Carbon GmbH, synthetic graphite, particle size distribution D10 = 6.8 μm, D50 = 18.4 μm, D90 = 42.9 μm), 2 wt. % carbon black (Imerys, C-Nergy Super C65), 2 wt. % CMC (sodium carboxymethylcellulose; Nippon, Sunrose MAC 500LC), and 2 wt. % SBR (styrene–butadiene rubber; Zeon, BM-451B). Here, graphite acts as the active material. Carbon black, CMC, and SBR provide the binder phase in this case. With the help of the binder material CMC and SBR, the powdered active material is coated on a 10 μm thick copper foil. To prepare the electrode, an electrode slurry with a solid content (graphite, CMC, SBR, and carbon black) of 48 wt. % was dissolved in water and applied to the copper foil by doctor blade coating. After coating, the electrode has a capacity of 3.3 mAh/cm^2. In the next step, the electrode is dried and calendered. Thereafter, the electrode has a layer thickness of the active material layer of 68 μm, which corresponds to a layer density of 1.4 g/cm^3.

Laser system

The laser processing was conducted using a TruMicro 2000 ultrashort pulse laser from TRUMPF. The laser system operates at a wavelength of 1030 nm. Scanner optics were used to precisely position the laser focus on the surface. An optical focusing system with a focal length of 160 mm focused the beam to a diameter of about 45 μm on the surface. In order to obtain a uniformly flat surface, the foil-like samples were fixed with the use of a vacuum plate. For analysis of the influence of pulse duration, the process was performed with pulse durations from 0.4 to 20 ps. Furthermore, the peak fluence was varied in a range from 0.72 to 6.49 J/cm^2. For each parameter, a field of 3 × 3 mm^2 was processed with holes that have a hole-to-hole distance of 100 μm and are arranged in a checkerboard shape. To analyze the influence of pulses per hole, 2–50 pulses per hole were used for each parameter combination. To avoid interaction between multiple pulses on one hole, hole fields were processed sequentially by multipass processing. This means that all holes were always perforated with one pulse before another pulse was applied.

Analysis of the ablation depth

The analysis of the ablation depth was carried out using a white light interferometer (WLI) NewView 8300 from the company Zygo. For this purpose, an area of 750 × 750 μm was measured in order to be able to analyze 49 hole geometries. The recorded measurement data were further analyzed by MATLAB to achieve a high throughput analysis. As shown in Fig. 1, a depth histogram was created from the measurement data. Using this histogram, the average surface area was determined at the upper maximum, as shown on the right lower part of Fig. 1. The bottom of the hole was then analyzed using the lowest maximum at the lower end of the histogram. To verify the procedure, comparative measurements were carried out using white light interferometer software MX^{TM}.

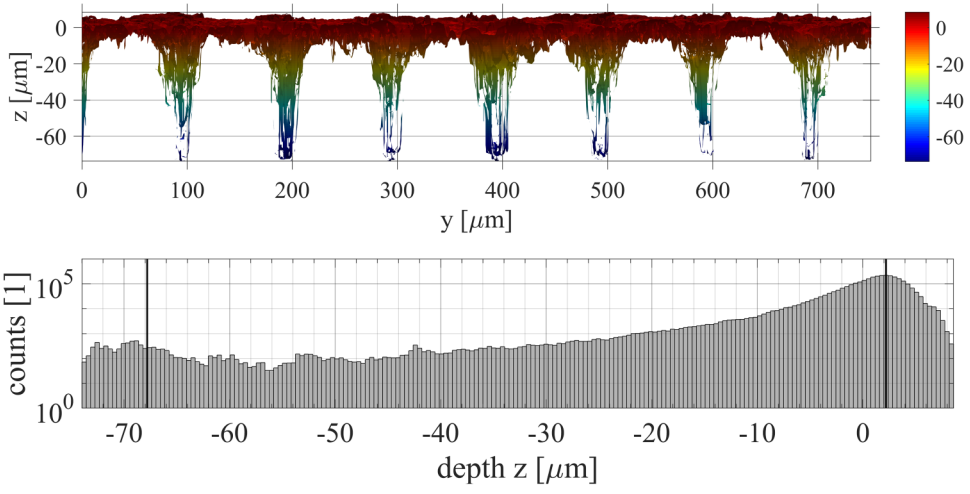

FIG. 1. Exemplary analysis of the hole depth by the 3D-WLI image (upper) and using a histogram of the depth distribution (lower).

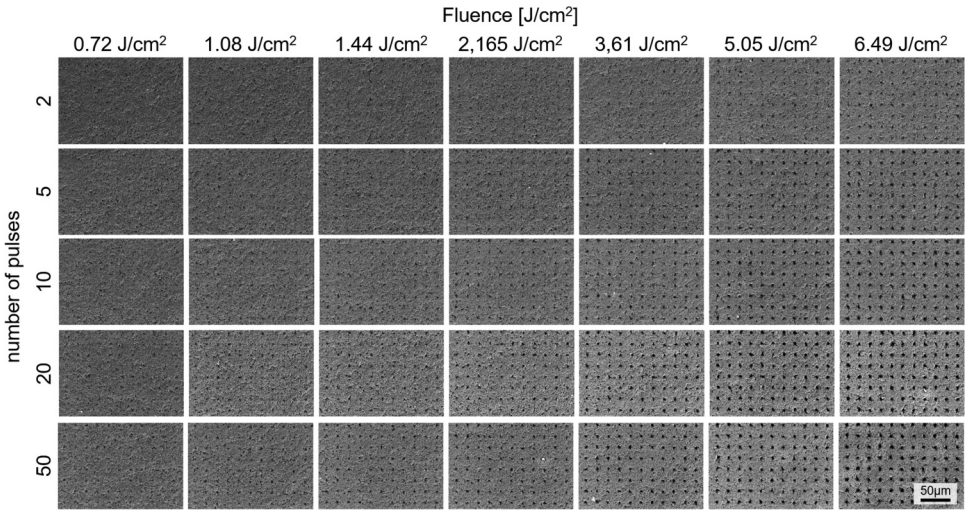

FIG. 2. SEM—top view picture of perforated electrodes with $t_H = 1$ ps.

Furthermore, surface images of the perforated fields were taken with a ZEISS Sigma 300VP scanning electron microscope. These surface images can be used to analyze visible changes in the processing field even below the measurable removal threshold.

Another difficulty, especially for processing with low fluences, can be seen in the surface roughness. White light interferometer measurements of the unmachined samples showed a maximum surface roughness Sz of about 12 μm. Since the roughness must be exceeded for a robust analysis of the ablation depth, even considering the SEM images, the measurement results of all pulse durations at 0.77 J/cm^2 with 2, 5, 10, 20, and 50 pulses as well as at 1.08 J/cm^2 with 2, 5, and 10 pulses were, therefore, ignored in the analysis. The ablation depth analysis for the above parameter constellations all showed no evaluable perforation depths, which were in the magnitude of the roughness.

RESULTS AND DISCUSSION

Ablation threshold

As already mentioned above, the well-visible ablation (in the SEM images) starts at a fluence of about 2 J/cm^2. In lower fluence regimes, ablation can be suspected on the top view images, but this ablation is not detectable in the measurements or is smaller than the surface roughness. In Fig. 2, the SEM top view images at 1 ps are shown. Here, it is clearly visible that ablation is already starting to become visible at 1.44 J/cm^2 and 50 pulses per hole. The transition between visible ablation and nonvisible ablation shifts toward higher fluence regimes at lower pulse numbers per hole. This effect is also observed in the WLI depth measurements.

However, it is also possible that ablation is already taking place in the lower fluence regime, but is too small for depth measurements and is thus below the roughness limit of approximately 12 μm of the unmachined surface. Since the analysis of the ablation in this area is not possible without errors, no clear statement can be made about the threshold fluence. Shirk *et al.* give a threshold fluence for graphite of 0.25 J/cm^2.[12] This threshold is below the fluence regime investigated in this study.

From the fluence of 2 J/cm^2 on, a measurable ablation begins, which is shown in Fig. 3 for a pulse duration of 1 ps and for five and 20 pulses per hole. It can be seen that for approximately 1 J/cm^2 the measured depth is still in the range of the surface roughness. From the mentioned 2 J/cm^2 also the difference between five and 20 pulses is clearly visible. Actually, it would be expected that the ablation at 20 pulses is significantly higher than that of five pulses. The slope of the two progressions differs slightly, with the gradient being a bit higher for 20 pulses per hole. However, both progressions show a nearly linear progression up to a fluence of 5 J/cm^2. From this fluence on, the ablation with 20 pulses is increasing disproportionately compared to the progression with five pulses. The ablation increases here up to 66 μm, which corresponds approximately to the coating thickness. Since this behavior is observed for all investigated pulse durations, an effect of smaller active material particles in this range can be excluded, and the increase in the ablation depth must be due to the high fluence of 6.49 J/cm^2.

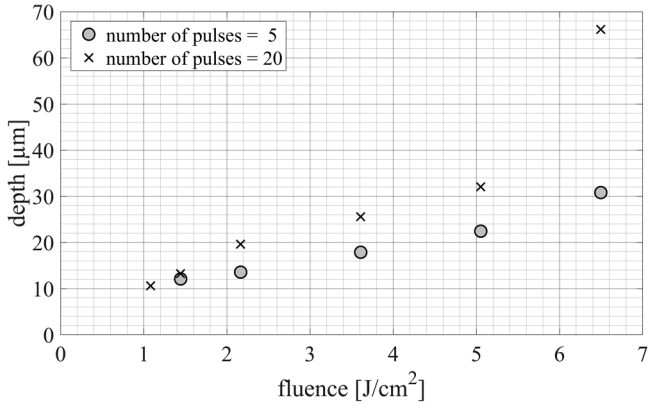

FIG. 3. Ablation depth for five and 20 pulses per hole at $t_H = 1$ ps.

Influence of number of pulses and fluence

The influence of the number of pulses was analyzed on the basis of three fluences. The measurement results for the hole depth are shown in Fig. 4. All three fluences shown here were selected since a depth measurement could be carried out with all numbers of pulses per hole. At the beginning with two pulses per hole, the measurement points are still very close to each other. All three curves show a linear increase in the beginning in which there is a linear correlation between the number of pulses and the hole depth. In the further progression, a tipping point can be seen in all three curves. This occurs for the two lower fluences in the range of 10–20 pulses per hole. After this tipping point, the course flattens out and the depth, however, seems to decrease again. In addition to the results shown here at $t_H = 1$ ps, this behavior is also visible for all other pulse durations that were analyzed. The fact that the ablation depth approaches a limit value can be explained by the enlarged focal area of the pulse. Since the intensity distribution within the focus is Gaussian, a larger volume is ablated in the center of the pulse than in the outer area of the pulse. This results in a cone-shaped and downward tapering cavity. When a second or subsequent pulse now arrives, the pulse will no longer arrive on a flat or slightly rough surface but on the cone described above, which was created by the previous pulse. Each additional incoming pulse enlarges this cone in depth and diameter, whereby the contact surface for the successive pulse thus increases significantly.[13] A constant pulse energy and an increasing area in the hole result in a decreasing fluence. At a certain point, the incident fluence is, therefore, no longer sufficient to enable material removal → the threshold fluence is no longer passed. From this point on, the hole cannot be drilled any deeper by increasing the number of pulses, and an equilibrium depth is reached, which is the case at fluences of 3.60 and 5.05 J/cm^2 in the range of 10–20 pulses.

At a fluence of 6.49 J/cm^2, the progression shows a significantly higher gradient. Due to the increased fluence, a greater depth is reached per pulse. In addition, the depth continues to increase up to 20 pulses. The tipping point in the curve thus shifts slightly to the right to higher pulse numbers. However, the hole depth increases to over 65 μm, which corresponds approximately to the layer thickness. A hole depth of 66.14 μm is already reached with 20 pulses. This means that the active material layer is already completely perforated at this point. Further pulses, subsequently, ablate the copper foil, thus the hole depth increases further. Nevertheless, the removal of copper is significantly slower than for the multimaterial investigated here, which describes the flattening of the course.

The results shown in Fig. 4 illustrate not only the influence of the number of pulses, but also the significant influence of the fluence upon the hole depth. For example, to achieve a hole depth of more than 40 μm, it is not sufficient in this case to increase the number of pulses. Even when using 50 pulses, this depth cannot be achieved at a fluence of <5.05 J/cm^2. In contrast, by increasing the fluence to 6.49 J/cm^2, this depth can already be achieved with 10 pulses. This means that, in terms of productivity and process speed, the fluence parameter is preferable to the number of pulses. However, it must also be mentioned here that increasing the fluence is not the only way to achieve a target depth. As can be seen in Fig. 4, there is no measurable difference in the depths of the present fluences with only two pulses. The differences become apparent within a few pulses where the fluence has a significant influence. As mentioned above, the data shown in Fig. 4 are representative of the other pulse durations investigated.

Dependency of the hole depth on the pulse duration

For ablation of metals or graphite, a clear dependence between ablation threshold and pulse duration is found in the literature.[12,14] It is shown that for metals, a short pulse duration has the lowest threshold fluence. By increasing the pulse duration, a slight increase in the threshold fluence occur. This behavior is not evident in the present study. For this purpose, perforated samples with a pulse duration of $t_H = 1$ ps, 10 pulses per hole, and three fluences were investigated. The fluences used were 2.16, 3.60, and 5.05 J/cm^2. These fluences were selected from the middle fluence range since

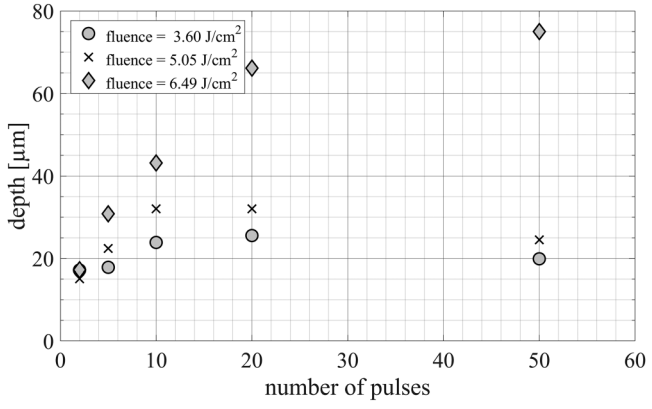

FIG. 4. Ablation depth over the number of pulses for 3.60, 5.05, and 6.49 J/cm^2 at 1 ps.

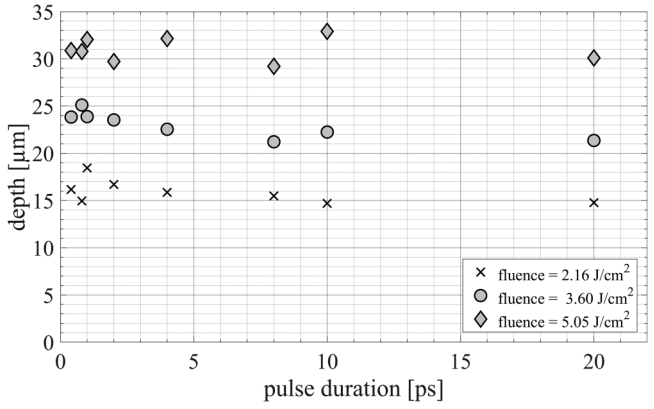

FIG. 5. Ablation depth over pulse duration for different fluence, 10 pulses per hole.

there is already a consistent ablation of material, but the layer is not ablated in its entirety. In addition, 10 pulses per hole were selected for the analysis because, as already described above, this area is still in the linearly increasing range. This excludes the possibility of additional effects influencing the results due to a high number of pulses without significant material removal.

On the basis of the results shown in Fig. 5, no significant influence on the pulse duration can be identified. The measured values of the ablation depth for 10 pulses per hole per fluence are in a similar range. From the graph, however, the large influence of the fluence can be seen again, which clearly exceeds the influence of the pulse duration in addition to the number of pulses.

CONCLUSION

In the present study, investigations were carried out on the perforation of graphite anodes. An ultrashort pulse laser with a wavelength of 1030 nm and a flexible pulse duration of 0.4–20 ps was used. The following parameters were analyzed: number of pulses, fluence, and pulse duration.

- For moderate fluences of <5 J/cm^2 and a low number of pulses, the depth of the hole can be linearly increased by increasing the number of pulses per hole. From 10 pulses per hole, an asymptotic progression of the depth is observed.
- At high fluences of >5 J/cm^2, the ablation depth continues to increase even after 10 pulses per hole. However, at this fluence range, the ground substrate can also be damaged by further pulses.
- No significant influence of pulse duration for perforating graphite electrodes was detected.
- The parameter fluence has a higher influence on the ablation depth than the number of pulses.
- At high fluence, the entire layer can be perforated with just a few pulses. In our case, 20 pulses at a fluence of 6.49 J/cm^2 were sufficient.

ACKNOWLEDGMENTS

This work was supported by the German Federal Ministry of Economic Affairs and Energy by funding the project "structur. E—Strukturierte Anoden für verbesserte Schnell-ladefähigkeit und Steigerung der Energiedichte von Lithium-Ionenbatterien" (No. 03ETE018F) and Project No. SGS-2022-007.

AUTHOR DECLARATIONS

Conflicts of Interest

The authors have no conflicts to disclose.

Author Contributions

Max-Jonathan Kleefoot: Conceptualization (lead); Methodology (lead); Visualization (equal); Writing – original draft (equal). **Jens Sandherr:** Formal analysis (equal); Visualization (equal); Writing – original draft (equal). **Marc Sailer:** Conceptualization (supporting); Formal analysis (equal); Writing – review & editing (equal). **Sara Nester:** Investigation (supporting); Visualization (equal); Writing – review & editing (equal). **Jiří Martan:** Investigation (supporting); Methodology (equal); Writing – review & editing (equal). **Volker Knoblauch:** Methodology (equal); Writing – review & editing (equal). **Malte Kumkar:** Investigation (supporting); Resources (equal); Writing – review & editing (equal). **Harald Riegel:** Conceptualization (supporting); Supervision (equal); Writing – review & editing (equal).

REFERENCES

[1]J. Proell, R. Kohler, A. Mangang, S. Ulrich, C. Ziebert, and W. Pfleging, "3D structures in battery materials," J. Laser Micro/Nanoeng. **7**, 97–104 (2012).
[2]W. Pfleging, "Recent progress in laser texturing of battery materials: A review of tuning electrochemical performances, related material development, and prospects for large-scale manufacturing," Int. J. Extreme Manuf. **3**, 012002 (2021).
[3]R. Dubey, M-D Zwahlen, Y. Shynkarenko, S. Yakunin, A. Fuerst, and M. V. Kovalenko, "Laser patterning of high-mass-loading graphite anodes for high-performance Li-ion batteries," Batter. Supercaps **4**, 464–468 (2021).
[4]T. Tsuda, N. Ando, K. Matsubara, T. Tanabe, K. Itagaki, Soma, N. Susumu Nakamura, Narumi Hayashi, T. Gunji, T. Ohsaka, and F. Matsumoto, "Improvement of high-rate charging/discharging performance of a lithium ion battery composed of laminated $LiFePO_4$ cathodes/graphite anodes having porous electrode structures fabricated with a pico-second pulsed laser," Electrochim. Acta **291**, 267–277 (2018).
[5]K.-H. Chen, M. J. Namkoong, V. Goel, C. Yang, S. Kazemiabnavi, S. M. Mortuza, E. Kazyak, J. Mazumder, K. Thornton, J. Sakamoto, and N. P. Dasgupta, "Efficient fast-charging of lithium-ion batteries enabled by laser-patterned three-dimensional graphite anode architectures," J. Power Sources **471**, 228475 (2020).
[6]W. Pfleging, "A review of laser electrode processing for development and manufacturing of lithium-ion batteries," Nanophotonics **7**, 549–573 (2018).
[7]J. B. Habedank, J. Endres, P. Schmitz, M. F. Zaeh, and H. P. Huber, "Femtosecond laser structuring of graphite anodes for improved lithium-ion batteries: Ablation characteristics and process design," J. Laser Appl. **30**, 032205 (2018).
[8]J. B. Habedank, J. Kriegler, and M. F. Zaeh, "Enhanced fast charging and reduced lithium-plating by laser-structured anodes for lithium-Ion batteries," J. Electrochem. Soc. **166**, A3940–A3949 (2019).
[9]W. Pfleging, R. Kohler, and J. Pröll, "Laser generated microstructures in tape cast electrodes for rapid electrolyte wetting: new technical approach for cost efficient battery manufacturing," Proc. SPIE 8968, 89680B (2014).
[10]J. Meijer, K. Du, A. Gillner, D. Hoffmann, V. S. Kovalenko, T. Masuzawa, A. Ostendorf, R. Poprawe, and W. Schulz, "Laser machining by short and ultrashort pulses, state of the art and new opportunities in the age of the photons," CIRP Ann. **51**, 531–550 (2002).
[11]S. Mishra and V. Yadava, "Laser beam micromachining (LBMM)—A review," Opt. Lasers Eng. **73**, 89–122 (2015).
[12]M. D. Shirk and P. A. Molian, "Ultra-short pulsed laser ablation of highly oriented pyrolytic graphite," Carbon **39**, 1183–1193 (2001).
[13]D. Holder, R. Weber, T. Graf, V. Onuseit, D. Brinkmeier, D. J. Förster, and A. Feuer, "Analytical model for the depth progress of percussion drilling with ultrashort laser pulses," Appl. Phys. A **127**, 59 (2021).
[14]J. Winter, M. Spellauge, J. Hermann, C. Eulenkamp, H. P. Huber, and M. Schmidt, "Ultrashort single-pulse laser ablation of stainless steel, aluminium, copper and its dependence on the pulse duration," Opt. Express **29**, 14561–14581 (2021).